

# Laboratory Essay with Online Back-calculation Anti-windup Scheme for a MTG System

Antônio M. S. Neto, Thaise P. Damo, Antonio A. R. Coelho

Federal University of Santa Catarina, Department of Automation and Systems, 88040900  
Florianopolis, SC, Brazil (e-mail: antoniosalla@gmail.com, thaisedamo@gmail.com, aarc@das.ufsc.br)

**Abstract:** This paper describes a lecture based on a laboratory experiment of the under-graduate course of Control and Automation Engineering at the Federal University of Santa Catarina. The goal is to show to the students the differences, codes and performance of tuning methods for the PID controller implemented with online back-calculation anti-windup scheme applied to a MTG (motor+tacogenerator) plant. The assessed system is used in many activities of a laboratory discipline of Feedback Systems. The whole study is conducted with a real plant instead of relying on computational numerical simulation. Analyzed tuning methods are: Ziegler-Nichols, Chien-Hrones-Reswick, Åström-Hägglund, AMIGO. Finally, the PID, tuned by the Internal Model Control (IMC), is also evaluated for different filter design parameters. The online experiment gives a better understanding, for the students, of how different tuning methods modify the system stability and the magnitude of the control signal.

**Keywords:** PID controllers, control system analysis, anti-windup, back-calculation, educational.

## 1. INTRODUCTION

Industrial processes are subjected to restrictions. For example, a controller operates in a limited range of 1 to 5 V or 4 to 20 mA, a valve cannot be opened more than 100% and less than 0% or a motor working as an actuator has a speed limit. These constraints represent operation limitations on the process. As a result, the real input signal is temporarily different from the output signal of the controller. When this happens, if the controller is initially designed to operate in a linear region, the behavior of the closed-loop system dynamic deteriorates as compared to the expected linear performance. This inadequate behavior (saturation of the direct-loop) is called windup. Figure 1 illustrates a closed-loop control system with an ideal PID controller and a limitation of magnitude on the control effort.

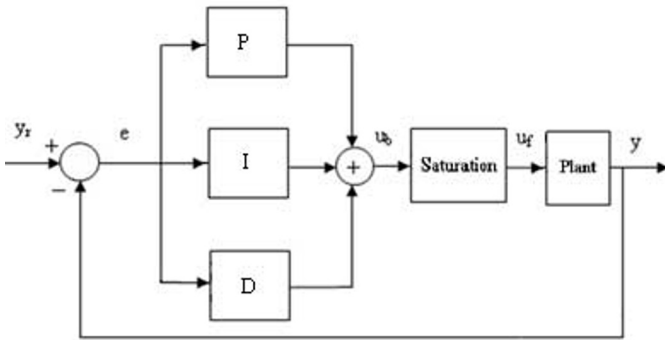


Fig. 1 – Closed-loop control system: constraint case.

The classical form of the saturation on the magnitude of the control signal, shown in Figure 1, is described by the following equation:

$$u_f = \begin{cases} u_{\max}, & u_b > u_{\max} \\ u_b, & u_{\min} \leq u_b \leq u_{\max} \\ u_{\min}, & u_b < u_{\min} \end{cases} \quad (1)$$

where the signals  $u_b$  and  $u_f$  are, respectively, the controller output and the real input of the process.

To understand the windup phenomenon in a control-loop, let us consider the second-order continuous system represented through the following model:

$$G_p(s) = \frac{1}{(s+1)(5.17s+1)} \approx \frac{e^{-s}}{(5.17s+1)} \quad (2)$$

controlled by a PI+D controller with and without the presence of saturation in the control signal ( $u_{\min} = 0$  V,  $u_{\max} = 5$  V). This simulation can be conducted at Simulink or ScicosLab computational platforms. Modeling the system by a first-order differential equation,  $K_p = 1$ ,  $\tau = 5.17$  s,  $\theta = 1$  s, and applying the first rule of Ziegler-Nichols tuning, it is possible to set the following parameters:  $K_c = 6.204$ ,  $T_i = 2$ ,  $T_d = 0.5$ . Figures 2 and 3 show the step response for a setpoint tracking of magnitude 2.5. The closed-loop control system with saturation presents an excessive overshoot and a long settling time when compared with the case without saturation (observe that saturation effectively opens the loop). Therefore, this simple example shows that the nonlinear dynamic of the actuator deteriorates the performance of the closed-loop control system and, a control structure modification on the design of the PI+D controller is necessary to avoid, for example, the actuator wear and an inappropriate loop behavior.

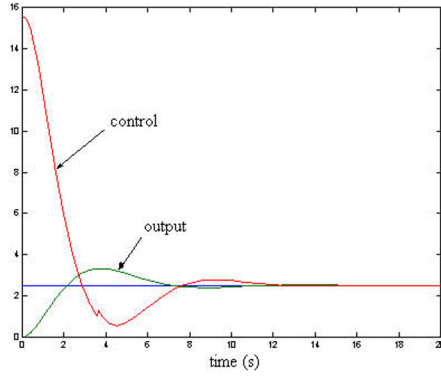


Fig.2 – Closed-loop step response with PID controller without saturation.

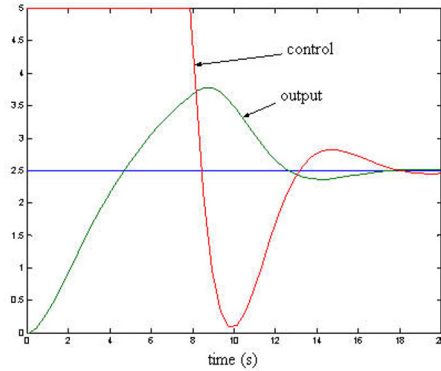


Fig. 3 – Closed-loop step response with PID controller with saturation.

Assuming that control education must be conceptual and experimental and as an attempt to give the practical loop characteristics of the PID tuning in the back-calculation anti-windup scheme, this paper shows a laboratory lecture of a discipline, called Feedback Systems, at the Federal University of Santa Catarina of an under-graduate course in Control and Automation Engineering. The goal is to give to the students not only ideas of the system stability aspects using different PID tuning sets but also online numerical code, energy factor of the control signal and loop saturation using setpoint changes.

In addition, the PID controller is the most adopted controller in the industry because of its preferable cost/benefit ratio when compared to other control techniques. The study of forms of configuration and parameter tuning are important aspects for teaching in engineering courses (Ang et al., 2005; Åström and Hägglund, 2006).

## 2. ANTI-WINDUP TECHNIQUE

Valves and motors as actuators present operating limits. When the control signal reaches the maximum or minimum limit of the actuator, control saturation happens. This phenomenon makes the feedback-loop inaccurate, because the actuator remains on its maximum or minimum limit independently of the process output. The consequence is that the transitory response becomes oscillatory, which is extremely unsatisfactory in industrial processes. If a controller with integral action is utilized, the error continues

to be integrated and the integral term becomes too big, this means, continues to be greatly increased (windup). For the controller to come back to operate in the linear region it is necessary to decrease the integral term. So, it is expected that the error measurement changes its signal and, for a long period of time, apply in the controller input a signal of opposite error. There are several ways to avoid the integrator windup. Next, is reviewed the popular technique called back-calculation (with the basic idea of stopping the integrator being continuously increased when the saturation happens). Figure 4 illustrates the block diagram of the anti-windup PID controller with back-calculation scheme.

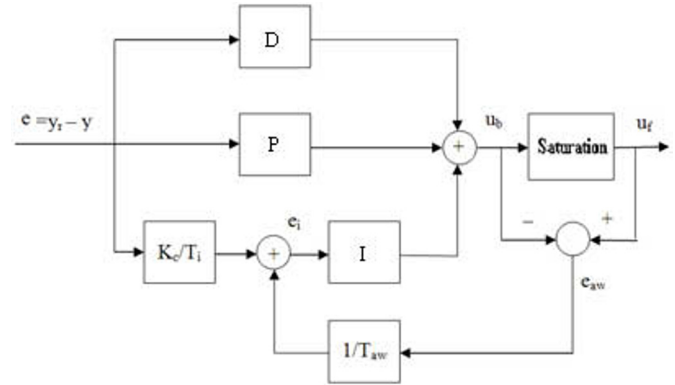


Fig.4 – Anti-windup PID controller topology.

The basic idea of the back-calculation technique is: when the output of the actuator saturates, the integral term is again calculated in a way that its value stays inside the linear limit of the actuator. It is advantageous making this correction not instantly, but dynamically with a time constant  $T_{aw}$ .

In Figure 4, the system presents an additional feedback-loop. The difference between the input and the output of the actuator constitutes an error  $e_{aw}$  that is added to the input of the integrator with a gain of  $1/T_{aw}$ . When the saturation does not exist, the error  $e_{aw}$  is null and the controller is operating in the linear region. In other words, the signal  $u_f$  is not saturated. If there is saturation,  $e_{aw}$  is different from zero. The time taken by the integrator input to tend to zero is determined by the gain  $1/T_{aw}$ , where  $T_{aw}$  can be interpreted as the time constant that determines how fast the input of the integrator becomes zero. The selection of small values for  $T_{aw}$  can be advantageous. However, a small value choice for  $T_{aw}$  should be carefully made, especially for systems with derivative action. What may happen is that the measurement noise can take the output of the controller into saturation state, resulting in a fast actuation of the anti-windup loop and making the input of the controller undesirably zero. In practice,  $T_{aw}$  should be bigger than  $T_d$  and smaller than  $T_i$ . An empiric selection rule suggested is  $T_{aw} = \sqrt{T_i T_d}$  or  $T_{aw} = T_i$  (Åström and Hägglund, 1995; Visioli, 2006).

Figures 5 and 6 show the step response for a setpoint with magnitude 2.5, using the system model as in (1), where the plant is controlled by a PI+D controller ( $K_c = 6.204$ ,  $T_i = 2$ ,  $T_d = 0.5$ ,  $T_{aw} = 1$ ) assessed with and without the anti-windup

compensation. The control system with anti-windup presents small oscillation and better settling time.

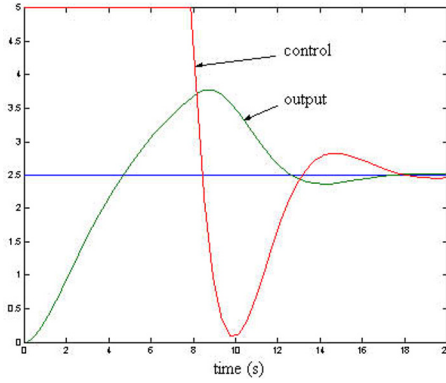


Fig. 5 – Closed-loop dynamic with PID controller without anti-windup.

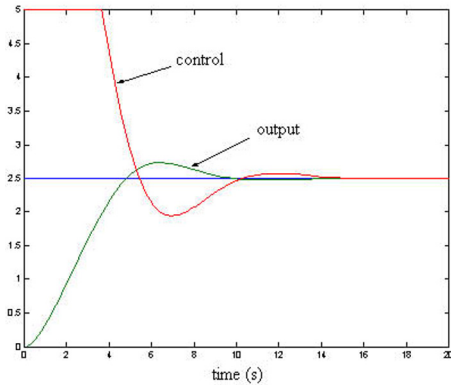


Fig. 6 – Closed-loop dynamic with PID controller with anti-windup.

The anti-windup technique provides a shorter saturation time in the control signal. This is advantageous from the operating viewpoint, it means, improves the closed-loop stability, reduces the wear of instrumentation and extends the actuator life-time. There are many references explaining the theory of anti-windup techniques, which can provide a more formal description and insight about the implementation (Bohn and Atherton, 1995; Peng et al. 1996).

### 3. PID CONTROLLER EVALUATION ON A PRACTICAL ESSAY

The experimental plant, called MTG, to be utilized in the analysis of the PID controller with the objective of reducing the windup effect in the control loop, consists of a DC motor coupled by a small belt to another DC motor which is responsible for generating the tachometer voltage (speed measurement), as shown in Figure 7.

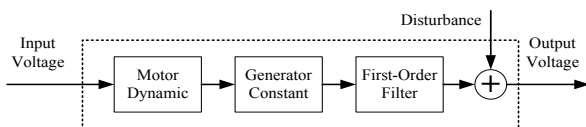


Fig. 7 – MTG experimental prototype.

The input signal for the plant is a voltage for the DC motor and the output is also a voltage corresponding to the angular speed. The voltage is ranging from 0 to 5 V and the sampling period is 0.1 s. Plant model parameters are calculated from an experimental essay (step response) with the control magnitude of 3 V, as shown in Figure 8.

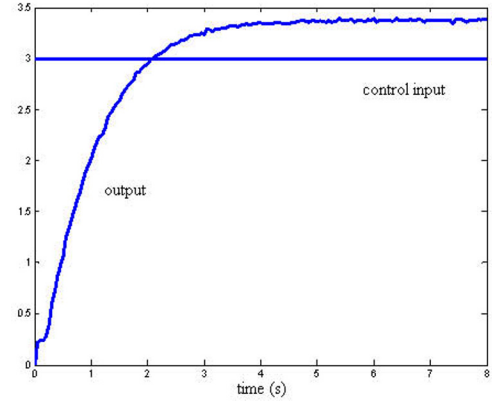


Fig. 8 – MTG response for a step of 3 V.

The estimated model that represents the MTG dynamic is given by

$$\frac{V_{out}(s)}{V_{in}(s)} = G_p(s) \approx \frac{K_p e^{-0s}}{(\tau s + 1)} \approx \frac{1.2e^{-0.1s}}{(1.1s + 1)} \quad (3)$$

Table 1 illustrates the implementation, in a machine cycle, the real-time PID controller with saturation and without anti-windup technique. The control law, before the saturation,  $u_b$  is calculated by the following parts: proportional, integral and derivative bands are given by  $u_p$ ,  $u_i$  and  $u_d$ . Since the aim is to teach experimental PID control education and to have the PID structure in Figures 1 and 2 realizable, the integral part is adjusted with the forward rectangular approach while the derivative with the first-order difference (Bobál et al., 2005).

Table 1 – Basic cycle of the PID signal with saturation

```

e(k) = yr(k) - y(k);
up(k) = kc*e(k);
ui(k) = ui(k-1) + ((kc*ts)/ti)*e(k-1);
ud(k) = ((kc*td)/ts)*(e(k) - e(k-1));
ub(k) = up(k) + ui(k) + ud(k);
if ub(k) <= umin;
    uf(k) = umin;
elseif ub(k) >= umax;
    uf(k) = umax;
else
    uf(k) = ub(k);
end

```

Table 2 describes the classical tuning methods for implementation of the PID controller and with  $T_{aw} = \sqrt{T_i T_d}$  (O'Dwyer, 2000).

**Table 2 – Classical tuning for the PID controller**

| Tuning Method        | $K_c$   | $T_i$  | $T_d$                                      |
|----------------------|---|--|--|
| Ziegler-Nichols      | $\frac{1.2\tau}{K_p\theta}$                                     | $2\theta$  | $0.5\theta$                                |
| Chien-Hrones-Reswick | $\frac{0.6\tau}{K_p\theta}$                                     | $\tau$   | $0.5\theta$                                |
| Åström-Hägglund      | $\frac{0.94\tau}{K_p\theta}$                                    | $2\theta$  | $0.5\theta$                                |
| AMIGO                | $\frac{1}{K_p} \left\{ 0.2 + 0.45 \frac{\tau}{\theta} \right\}$ | $\left\{ \frac{0.8\tau + 0.4\theta}{0.1\tau + \theta} \right\} \theta$ | $\frac{0.5\tau\theta}{(\tau + 0.3\theta)}$ |

Using the estimated model described in (3) and the tuning rules from Table 2, it is possible to obtain the gains of Table 3, for the PID controller (Åström and Hägglund, 2006).

**Table 3 – PID controller gains**

| Tuning Method        | $K_c$  | $T_i$  | $T_d$ | $T_{aw}$ |
|----------------------|--------|--------|-------|----------|
| Ziegler-Nichols      | 11     | 0.2    | 0.05  | 0.1      |
| Chien-Hrones-Reswick | 5.5    | 1.1    | 0.05  | 0.2345   |
| Åström-Hägglund      | 8.6167 | 0.2    | 0.05  | 0.1      |
| AMIGO                | 4.2917 | 0.4381 | 0.049 | 0.146    |

System responses for each tuning method are illustrated in Figures 9 to 12.

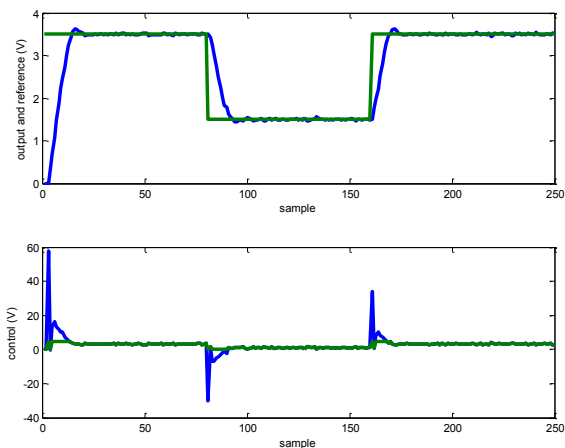


**Fig. 9 – System response to PID tuned by Ziegler-Nichols method.**

The Ziegler-Nichols tuning method provides the most aggressive control between the four methods. This kind of

behavior gives a large saturation area on the control signal with a short settling time.

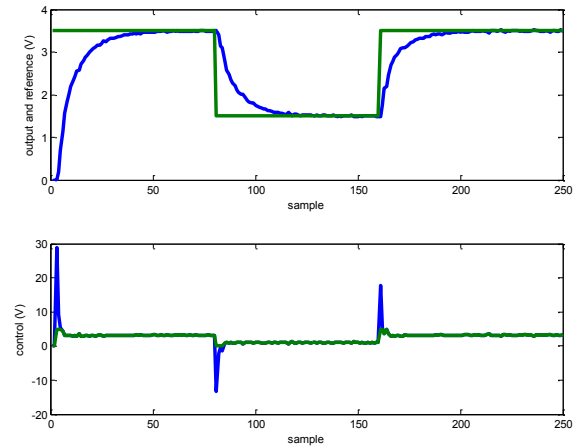


**Fig. 10 – System response to PID tuned by Chien-Hrones-Reswick method.**

The Chien-Hrones-Reswick tuning method does not present overshoot. It shows the longest settling time, the second less aggressive control and the lowest saturation area.

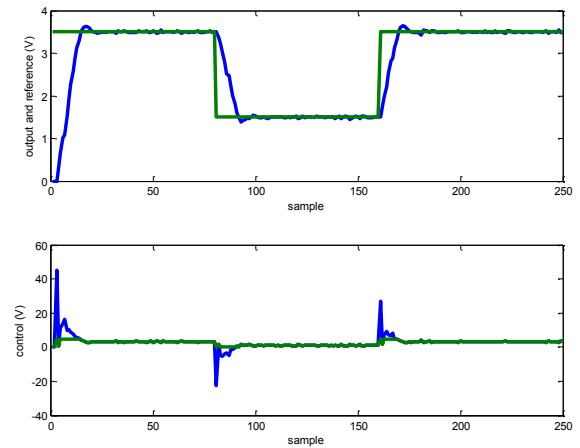


**Fig. 11 – System response to PID tuned by Åström-Hägglund method.**

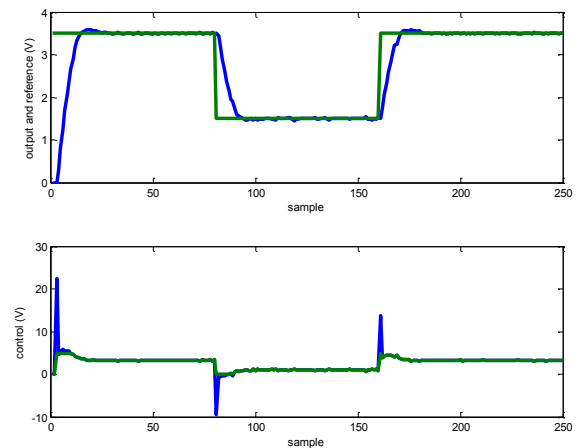


**Fig. 12 – System response to PID tuned by AMIGO method.**

The Åström-Hägglund tuning method presents a very similar response compared to the Ziegler-Nichols method but with a much less aggressive control. It also has less overshoot. The settling time and saturation area is very close to the Ziegler-Nichols method.

The AMIGO tuning method is the one that presents the second lowest saturation area between the four methods. The combination of parameters results in a good settling time according to the saturation area of the other methods. The settling time is still larger than the Ziegler-Nichols and Åström-Hägglund methods, but this is compensated by the smaller overshoot and the less aggressive control.

#### 4. IMC BASED PID TUNING

The IMC tuning method is becoming largely applied in the industry. So, essays based on the IMC-PID tuning method are presented as an alternative solution for the anti-windup PID strategy reviewed in this paper. This calibration method can provide good results not only decreasing the saturation level and overshoot of the system response but also by keeping the system speed at reasonable levels – more theoretical background of the IMC PID tuning can be found in Rivera et al. (1986) and Zulkeflee et al. (2010).

Next, the PID controller for the MTG plant is tuned by the IMC-PID settings. The goal of the control system is to achieve a fast and accurate setpoint tracking. IMC-PID tuning parameters for first-order plus dead-time processes are described in Table 4.

**Table 4 – PID controller settings with IMC strategy**

| PID Parameters | IMC Tuning  |
|----------------|---|
| $K_c$          | $\frac{\tau + 0.5\theta}{K_p(\lambda + 0.5\theta)}$ |
| $T_i$          | $\tau + 0.5\theta$                                  |
| $T_d$          | $\frac{\tau\theta}{2\tau + \theta}$                 |

Due to  $K_c$  being inversely related to the filter constant  $\lambda$  (associated with the plant response speed and the energy factor of the control), different essays with different values of  $\lambda$ , to verify the system response, are implemented. The parameter  $\lambda$  must be greater than  $0.8\theta$  because of the model uncertainty due to the Padé approximation. The integral time and derivative time of the PID controller are constants and with values  $T_i = 1.15$ ,  $T_d = 0.0478$ , respectively, and  $T_{aw} = 0.2345$ . Parameter  $K_c$  changes according to  $\lambda$  as displayed in Table 5.

**Table 5 – Parameter  $K_c$  of the PID according to  $\lambda$**

| $\lambda$ | $K_c$  |
|-----------|--------|
| 0.80      | 7.3718 |
| 9.70      | 0.9395 |

Closed-loop system results of the experiment, according to the variation of  $\lambda$ , are displayed in Figures 13 and 14.

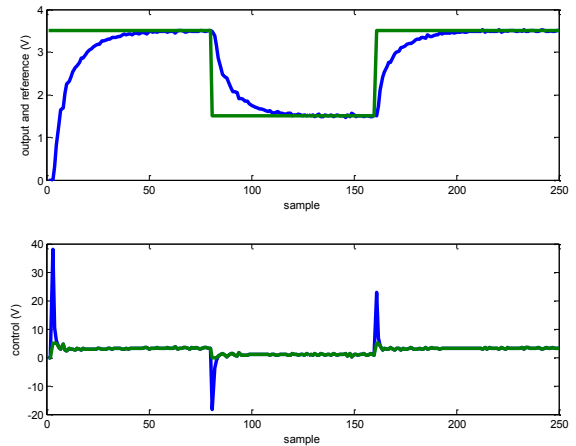


Fig. 13 – System response to PID tuned by IMC-PID method for  $\lambda = 0.8\theta$ .

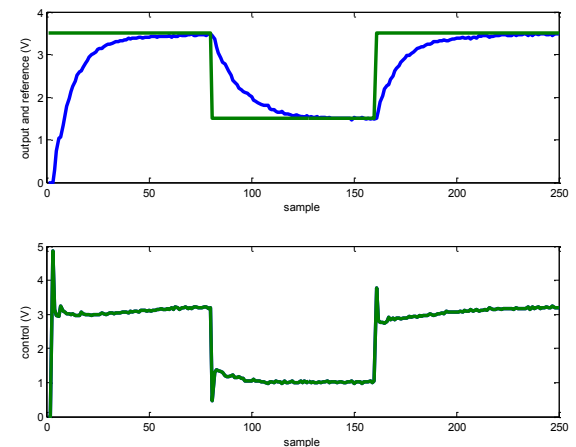


Fig. 14 – System response to PID tuned by IMC-PID method for  $\lambda = 9.7\theta$ .

Comparing the IMC-PID tuning with the other four methods displayed in Section 3, it can be observed that the saturation area is very small for greater values of  $K_c$  and almost absent for smaller values. The system also does not present overshoot for any value of  $\lambda$ . Comparing the results with the other method that presents no overshoot, Chien-Hrones-Reswick tuning, it is possible to note that the settling time of the IMC-PID tuning is smaller.

Utilizing  $\lambda = 9.7\theta$  the system achieved a control without saturation, but has slower behavior, and therefore, being the only method of the ones analyzed that can remove the saturation level on the control signal.

These experiments can be implemented with the Matlab numerical code presented in Appendix A.

#### 5. CONCLUSIONS

Through different tuning methods the process control engineering students can understand and observe how the

PID parameters affect the system dynamic under an on-line numerical code and anti-windup scheme. This practical case study, combined with the fact that the experiment is conducted over a real plant, not over a computer simulated model, opens the mind of the students on how a real system works, considering that an experimental system has measurement noise and does not have the exact behavior of the model obtained from the step response identification.

Costing less than some engineering textbooks, each university can build a MTG plant for control lab lessons and reinforcing classroom concepts. Another important point is that the numerical code and PID tuning methods presented in this paper do not apply only to the MTG plant, but for any stable system with first-order approximated behavior.

## ACKNOWLEDGMENT

This research was supported by the DAS of the Federal University of Santa Catarina and CNPq.

## REFERENCES

- Ang, K.H.; Chong, G.; Li, Y. (2005). PID Control System Analysis, Design, and Technology, *IEEE Trans. on Control Systems Technology*, pp. 559-576.
- Åström, K.; Hägglund, T. (1995). PID Controllers: Theory, Design, and Tuning, *ISA*.
- Åström, K.J.; Hägglund, T. (2006). *Advanced PID Control*, Instrument Society of America.
- Bohn C.; Atherton, D.P. (1995). An Analysis Package Comparing PID Anti-Windup Strategies, *IEEE Control Systems*, pp. 34-40.
- Bobál, V.; Böhm, J.; Fessl, J.; Macháček, J. (2005). *Digital Self-Tuning Controllers*, Springer.
- O'Dwyer, A. (2000). A Summary of PI and PID Controller Tuning Rules for Processes with Time Delay. Part 2: PID Controller Tuning Rules, *IFAC Digital Control: Past, Present and Future of PID Control*, pp. 211-216.
- Peng, Y.; Vrancic, D.; Hanus, R. (1996). Anti-Windup, Bumpless, and Conditioned Transfer Techniques for PID Controllers, *IEEE Control Systems*, pp. 48-57.
- Rivera, D.E.; Morari, M.; Skogestad, S. (1986). Internal Model Control: PID Controller Design, *Industrial & Engineering Chemistry Process Design and Development*, pp. 252-265.
- Visioli, A. (2006). *Practical PID Control*, Springer.
- Zulkeflee, S.A.; Shaari, N.; Aziz, N. (2010). Online Implementation of IMC Based PID Controller in Batch Esterification Reactor, *5<sup>th</sup> International Symposium on Design, Operation and Control of Chemical Processes*, pp.1612-1621.

## Appendix A. MATLAB SIMULATION CODE

| Matlab code of the PID controller  |
|--|
| clear all; close all; clc;<br>% ----- Initial conditions<br>nit = 250; ts = 0.1; umin = 0; umax = 4.9;<br>ub(1:3) = 0; uf(1:3) = 0; erro(1:3) = 0; y(1:3) = 0; |

```
up(1:3) = 0; ui(1:3) = 0; ud(1:3) = 0; eaw(1:3) = 0;
% ----- Reference
yr(1:80) = 3.5; yr(81:160) = 1.5; yr(161:250) = 3.5;
% ----- Plant model parameters
kp = 1.2; tau = 1.1; teta = 0.1;
lambda = 9.7*teta; % the IMC-PID tuning
% ----- PID controller parameters
method = 5; % Tuning method for the PID
switch method
case 1 % Ziegler-Nichols
kc = (1.2*tau)/(kp*teta); ti = 2*teta; td = 0.5*teta;
case 2 % Chien-Hrones-Reswick
kc = (0.6*tau)/(kp*teta); ti = tau; td = 0.5*teta;
case 3 % Åström-Hägglund
kc = (0.94*tau)/(kp*teta); ti = 2*teta; td = 0.5*teta;
case 4 % AMIGO
kc = (1/kp)*(0.2 + 0.45*(tau/teta));
ti = ((0.8*tau + 0.4*teta)/(0.1*tau + teta))*teta;
td = (0.5*tau*teta)/(tau + 0.3*teta);
case 5 % IMC-PID
kc = (tau+0.5*teta)/(kp*(lambda+0.5*teta));
ti = tau+0.5*teta;
td = tau*teta/(2*tau+teta);
end
taw = sqrt(ti*td);
% ----- Start the data acquisition board
inicializa_placa(5);
% ----- Closed-loop experiment
for k = 3:nit
% ----- Output and error
y(k) = recebe_dado(1);
erro(k) = yr(k) - y(k);
% ----- Control law with anti-windup
up(k) = kc*erro(k);
ui(k) = ui(k-1) + ((kc*ts)/ti)*erro(k-1) + ...
(ts/taw)*eaw(k-1);
ud(k) = ((kc*td)/ts)*(erro(k) - erro(k-1));
ub(k) = up(k) + ui(k) + ud(k);
% ----- Saturation
if ub(k) <= umin
uf(k) = umin;
elseif ub(k) >= umax
uf(k) = umax;
else
uf(k) = ub(k);
end
eaw(k) = uf(k) - ub(k);
% ----- Send control signal to the board
envia_dado(1,uf(k)); atraso_ms(1000*ts);
end
% ----- End the data acquisition board
finaliza_placa;
% ----- Simulation results
t = 1:nit;
subplot(2,1,1), plot(t,y(t),t,yr(t),'LineWidth', ...
3), ylabel('output and reference (V)'), xlabel('sample');
subplot(2,1,2), plot(t,ub(t),t,uf(t),'LineWidth', ...
3), ylabel('control (V)'), xlabel('sample');
```